

# An electron injector for the Electron-Ion Collider based on proton-driven plasma wakefield acceleration

J. P. Farmer,<sup>1,\*</sup> H. Jaworska,<sup>2,†</sup> A. Caldwell,<sup>1</sup> N. Lopes,<sup>3</sup>  
A. Pukhov,<sup>2</sup> L Reichwein,<sup>2,4</sup> F. Willeke,<sup>5</sup> and M. Wing<sup>6,7</sup>

<sup>1</sup>*Max Planck Institute for Physics, Garching, Germany*

<sup>2</sup>*Heinrich-Heine-Universität, Düsseldorf, Germany*

<sup>3</sup>*Instituto Superior Tecnico, Lisbon, Portugal*

<sup>4</sup>*Forschungszentrum Jülich, Jülich, Germany*

<sup>5</sup>*Brookhaven National Laboratory, Brookhaven, US*

<sup>6</sup>*UCL, London, UK*

<sup>7</sup>*DESY, Hamburg, Germany*

We describe an electron bunch injector scheme based on proton-driven plasma wakefield acceleration for the Electron-Ion Collider. The proton bunches needed to drive the plasma wake are taken from the existing Blue-Ring of RHIC. The polarized electron source is taken from the current EIC design. We describe the different elements making up the injection scheme and give an estimate for the performance. Our initial study indicates that the design parameters of the EIC are within reach when accelerating the electron bunches in the proton-driven plasma wake, with average polarization of  $\sim 70\%$  and a luminosity of  $10^{34}\text{ cm}^{-2}\text{ s}^{-1}$ .

## I. INTRODUCTION

The Electron-Ion Collider (EIC) is planned to be constructed at Brookhaven National Laboratory (BNL)[1]. The facility will make use of the existing infrastructure of the Relativistic Heavy Ion Collider (RHIC), in particular one of its two superconducting accelerator rings (see the schematic

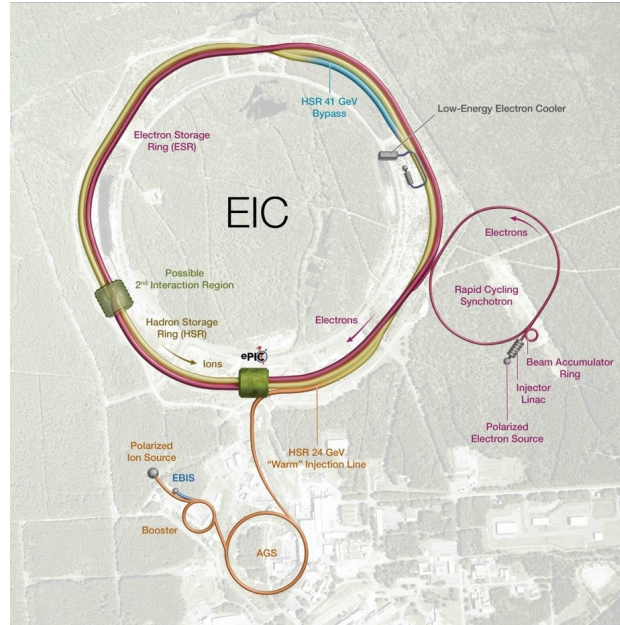


FIG. 1. The planned layout for the EIC accelerator complex.

\* j.farmer@cern.ch

† Helena.Jaworska@hhu.de

layout in Fig. 1). The EIC is designed to deepen our understanding of nuclear structure, provide insight into the phenomenon of increasing gluon density at low Bjorken- $x$  – also referred to as gluon saturation – and help resolve the longstanding question of the proton spin.

This ambitious scientific program requires a challenging accelerator design capable of supporting collisions between electrons with energies of up to 18 GeV and a wide range of ions, from protons to uranium, with energies of up to 275 GeV. In addition, the collider must deliver a high luminosity of up to  $L = 10^{34} \text{ cm}^{-2} \text{ s}^{-1}$ , provide polarized electron and light-ion beams with an average polarization of 70 %, support bunch-to-bunch polarization reversal, and operate over a center-of-mass energy range from 29 GeV to 140 GeV. Furthermore, the design must accommodate a multipurpose colliding-beam detector with particular emphasis on the detection of forward- and backward-scattered particles emerging from the interaction point.

These demanding requirements must be met at an affordable cost, which constitutes a significant challenge in itself. This motivates the exploration of novel technical solutions capable of delivering high performance at moderate cost. In this work, we report on a promising, cost-effective concept for an electron accelerator capable of providing electron beams up to 18 GeV. The concept exploits the existing second superconducting ring, originally intended for accelerating protons to 250 GeV, to drive a compact and comparatively inexpensive plasma wakefield accelerator. Such a system could accelerate electrons from energies of about 100 MeV to 18 GeV.

### A. EIC baseline design

We begin with an overview of the EIC baseline specification, against which the proposed scheme must be compared. The EIC baseline includes very high electron beam currents of up to 2.5 A and a high beam polarization, exceeding the equilibrium polarization achievable in a storage ring. Electrons are produced with a polarization of 85 % by the existing polarized gun. Their polarization is preserved during acceleration to the final energy before injection into the storage ring, where it decays toward the equilibrium polarization of approximately 50 %. Stored electron bunches are planned to be replaced with fresh bunches once their polarization drops below approximately 60 %. This quasi-continuous electron injection at a rate of about 1 Hz places strong demands on the capabilities of the electron injector. The corresponding electron beam parameters are summarized in Table I.

Parameter	Units	$E_{\text{beam}} = 10 \text{ GeV}$	$E_{\text{beam}} = 18 \text{ GeV}$
Electron Energy	GeV	10	18
Maximum Bunch Charge	nC	28	10.7
Number of bunches		1160	290
Beam Current	A	2.5	0.24
Initial Polarization	%	85	85
Average Polarization	%	70	70
Horizontal Emittance	nm	20	20
Vertical Emittance	nm	3.3	3.3
Energy loss per turn	MeV	4.01	42
RMS Energy Spread	$1 \times 10^{-4}$	5.5	10
Polarization Lifetime	min	406	20.4

TABLE I. Design parameters of the EIC electron beam.

## B. Overview of the proposed scheme

We consider a scheme similar to that developed by the Advanced Wakefield Experiment (AWAKE) Collaboration [2], discussed in Section I C, as the basis for an electron injector for the EIC. This is a first attempt to develop a proton-driven plasma acceleration scheme for the electron bunches for the EIC, which can then be optimized and worked out in more detail in the future should interest develop in pursuing this approach. We note that many of the challenges presented in the paper for the plasma-based acceleration part have been solved for the AWAKE case.

There are some differences between the proposed scheme and AWAKE, which we discuss here to set the stage for the following more detailed sections. In our approach, the proton bunches which drive the plasma wake are taken from the Blue-Ring of the RHIC complex, and the parameters taken for the proton bunch are given in Table II. A more detailed description of the proton bunch preparation scheme is presented in Section II A.

Parameter	Units	Value
Energy	GeV	275
Bunch population		$3 \times 10^{11}$
Number of bunches		1160
Bunch length	mm	50
Bunch waist	$\mu\text{m}$	200
Normalized transverse emittance	$\mu\text{m}$	2
Ring cycling time	min	11

TABLE II. The parameters of the proton bunches from the Blue-Ring taken in our studies.

The electron bunches are prepared using the existing polarized electron source [3]. There is an anti-correlation between the electron bunch charge and the maximum energy to which the electrons can be accelerated in the plasma. We have chosen  $E_e = 10$  GeV as the working point for our studies as this is expected to be the most difficult set of parameters to achieve given the requirement of high electron bunch charge. These considerations lead to the electron bunch parameters given in Table III.

Parameter	Units	Value
Energy entering plasma	MeV	150
Energy after plasma	GeV	10
Bunch charge	C	$1 \times 10^{-9}$
Bunch length	$\mu\text{m}$	90
Bunch waist	$\mu\text{m}$	11.5
Normalized transverse emittance	$\mu\text{m}$	10

TABLE III. The parameters of the electrons bunches taken in our studies.

Note that the electron bunch charge for one acceleration is approximately 28 times lower than the value required for EIC physics (see Table I). To achieve the required charge of 28 nC, we foresee using ‘top-up’ injection. i.e., a fresh bunch of 1 nC would be added to already circulating bunches at an average rate of  $\sim 1$  Hz. This can be accomplished by extracting proton bunches in bursts at, e.g., 20 Hz from the Blue-Ring for electron bunch acceleration. Given the proton ring cycling time, this allows for an average rate of 1.6 Hz of full-energy electron bunches for injection into the electron storage ring (ESR). Note that this would not only keep the needed bunch charge at the required level, but would also allow for maintaining a high average polarization of the electron bunch. The scheme for achieving these electron bunch parameters is described in Section II B, and the top-up injection scheme in Section IV B.

As with the AWAKE scheme, two plasma sections are necessary. The first section is used to modulate the proton bunch into a series of microbunches. The modulation process is seeded and the plasma is created using a short laser pulse. In contrast to the AWAKE scheme, we anticipate using a discharge plasma for the acceleration section. The plasma source descriptions are given in Section III C.

The electron bunch acceleration is performed in the second plasma source and has been studied using particle-in-cell simulations as described in Section III A. The studies are based on extensive developments performed in the context of the AWAKE experiment and are based on codes which have been verified to be accurate for this scheme of plasma wakefield acceleration. We note that it is not expected that the electron bunch polarization is degraded during the acceleration process. This is discussed below in some detail in Section III B. The electron bunches exiting the plasma must be fine tuned in energy to match the set energy of the ESR. This fine-tuning, as well as the top-up injection scheme into the ESR are described in Section IV.

We discuss the layout of the main components that would be necessary for this electron injector scheme in Section V, and discuss possible locations for installation in the EIC tunnel. We then conclude with a summary of the results found in our studies to date, and discuss ways in which the results could be enhanced.

### C. The AWAKE Experiment

Plasma can sustain high electric fields and can be used to produce accelerating gradients larger than in conventional particle accelerators [4–8]. First experiments relied on a laser pulse or an electron bunch to disturb the plasma and drive large fields in their wake. Proton drivers were proposed [9] as a means to reach high, TeV-level, energies in one plasma stage. These initial simulations relied on high-energy protons in short bunches of order  $100\ \mu\text{m}$ . Although the creation of short proton drive bunches is being actively pursued [10, 11], they are not currently available at any laboratory.

High-energy bunches of protons with lengths of  $\mathcal{O}(\text{cm})$  such as those at CERN, BNL and FNAL are available, although such bunches are expected to drive only weak wakefields. To overcome this, the self-modulation instability [12] can be utilised that divides a long driver bunch into a group of short so-called microbunches that can resonantly drive wakefields. The AWAKE [13, 14] experiment located at CERN investigates proton-driven plasma wakefield acceleration.

AWAKE uses protons from the CERN Super Proton Synchrotron (SPS) with energy of 400 GeV in bunches of  $3 \times 10^{11}$  protons and about 5 – 10 cm in length. Microbunches are formed in a controlled manner by using the ionization front of a high-power laser to seed the self-modulation mechanism [15]; alternatively, electron bunches can also be used to seed the self-modulation [16]. The strong wakefields driven by these microbunches are sampled by a witness bunch of electrons that is externally injected and accelerated to higher energies. The whole process currently takes place in a ten-metre-long rubidium plasma source of density in the range  $10^{14} - 10^{15}\ \text{cm}^{-3}$ . The plasma is created by ionising rubidium vapour at a temperature of about 200 °C. Initial experiments have shown a clear microbunching of the long proton bunch [17, 18] and acceleration of electrons from 19 MeV up to 2 GeV within the 10 m of plasma [17].

Future experiments at AWAKE [2] will focus on electron acceleration that is scalable to longer distances and with control of the electron bunch emittance. After these experiments, which will start in 2029, the AWAKE scheme should have been sufficiently demonstrated for application, such as that discussed here. The AWAKE experiment will therefore be upgraded to have two plasma sources (see Fig. 2), where the self-modulation of the proton bunch takes place in the first and electron acceleration in the second. Rubidium vapour will again be used for the first plasma source

at a default density of  $7 \times 10^{14} \text{ cm}^{-3}$ , but with the ability to introduce a step in the density that will stabilise the wakefields [19, 20]. Electron bunches will be injected on-axis in a 30-cm gap between the first and second plasma source. Electrons of 150 MeV in bunches of a few hundred pC in charge with an emittance of about 2 mm mrad and a duration 200 fs will be used. These much shorter electron bunches than currently used ( $> 4 \text{ ps}$ ) should lead to a significantly higher capture of electrons in the wakefields and a more controlled acceleration process. The second plasma source will be at least 10 m in length and could be based on laser-ionised rubidium vapour or a discharge plasma source using a noble gas, where a discharge source should in principle be scalable to lengths longer than is possible for a rubidium vapour source.

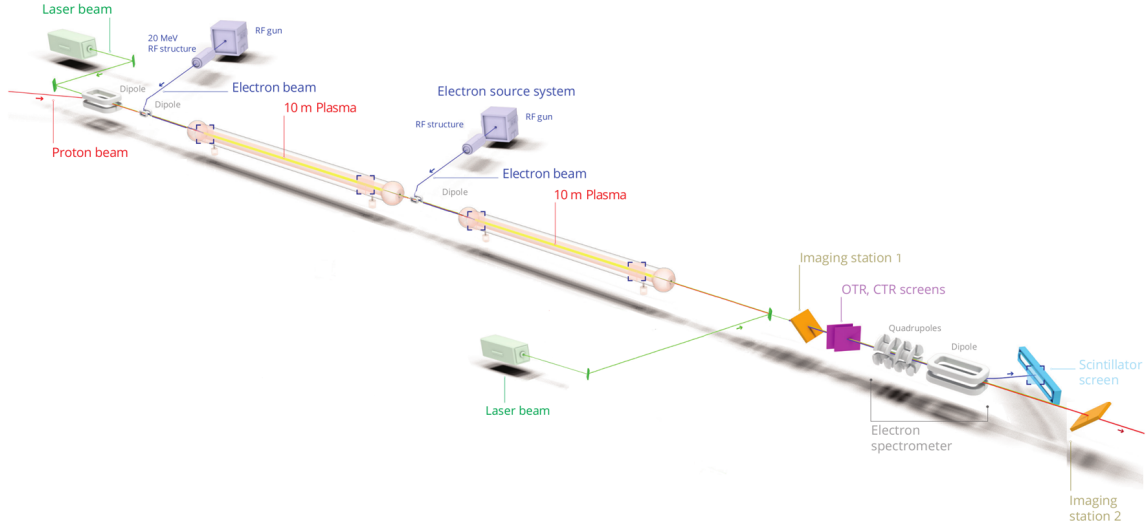


FIG. 2. Overview of the layout of future AWAKE experiments showing two plasma sources. In the first rubidium plasma source proton bunches can have the modulation seeded by a laser pulse or electron bunch. The second plasma source is shown here as laser-ionised rubidium but could also be a discharge plasma source. Various diagnostics are shown after the second plasma source.

The knowledge that has been and will be gained from the AWAKE experiment feeds directly into the design concept we envisage for the EIC electron injector.

## II. CONVENTIONAL ACCELERATORS

In the next sections, we describe the RF based accelerator components required to provide the input for the plasma acceleration scheme. These are the proton bunch accelerator to drive the plasma wake and the polarized electron bunch system needed to prepare the electron for acceleration in plasma.

### A. The proton accelerator

The RHIC Blue-Ring is an existing 250 GeV superconducting accelerator in the 3890 m tunnel, one of the two RHIC accelerator rings, that was considered not to be needed for the EIC. The Blue-Ring superconducting magnets are configured for clockwise particle motion, the direction of the EIC electron beam. With an upgraded RF system and power supply system it is envisioned to become the driver that will provide the 275 GeV proton beam that generates the plasma wakefield that accelerates an electron beam from 150 MeV to up to 18 GeV.

As stated in Table II, the proton driver will deliver  $n_b = 1160$  bunches of  $N_p = 3 \times 10^{11}$  protons at 275 GeV every  $T_{cycle} = 11$  min. This corresponds to a bunch current of  $I_b = 3.7$  mA and a total beam current of  $I_{total} = 4.3$  A. These performance requirements considerably exceed the beam parameters planned for the 275 GeV EIC Hadron Storage Ring (HSR), for which the bunch population is  $N_p = 6.3 \times 10^{10}$ , corresponding to  $I_b = 7.8$  mA,  $I_{total} = 0.9$  A. The bunch length of 50 mm and number of bunches for the proposed scheme is the same as the HSR, and the invariant longitudinal emittance is a factor two higher.

The EIC HSR proton beam is polarized and originates from an intensity-limited polarized proton source. The protons for the driver will be generated in an unpolarized  $H^-$  source that can provide four times the bunch intensity which allows us to assume the required driver proton bunch population will be possible. Such beam current will limit the 275 GeV storage time to less than a minute because of image current heating of the stainless steel beam pipe. The required longitudinal emittance is achieved because the transverse emittance of the round driver beam can be considerably relaxed compared to the flat collider proton beam,  $(\varepsilon_x \cdot \varepsilon_y)_{driver} = 10 \times (\varepsilon_x \cdot \varepsilon_y)_{collider}$ . The Alternating Gradient Synchrotron (AGS) accelerates the collider bunches in single-bunch mode due to the limitations of the polarized proton source. Using the  $H^-$  source, the AGS can accelerate six bunches in a 10 Hz cycle which will speed up the injection time to 120 s. The ramp time is limited by the time constants of the quench protection circuitry. With a modest improvement in the electronics, a ramp cycle time of 9 min can be achieved. Thus, the assumed driver cycling time of 11 min is possible.

We can conclude that Blue-Ring with some improvements in RF systems and cycle time will be able to provide the drive beam for plasma wakefield that accelerate 1 nC electron bunches for the ESR.

### B. The electron linac

The electron beams of the EIC are generated in an existing polarized source that has demonstrated 90 % polarized electron bunches up to 10 nC charge [3]. The source can be operated with a frequency of 28 Hz generating 1 nC electron bunches. A Wien-Filter will rotate the electron spin into the vertical directions and this direction is maintained during the entire accelerator process until injection into the ESR.

Electrons of 150 MeV are injected into the plasma acceleration channel. These electrons, after being extracted from the polarized source are injected into a 500 MHz bunching section followed

by a conventional s-band linac with three accelerating structures of 3 m length spaced by a 1 m drift to allow focusing and correction elements as well as utilities to be placed. The RF power is generated in three s-band klystrons and the RF pulse structure is generated in commercial solid states modulators. The structures generate an accelerating gradient of 16.6 MV/m.

This injector will provide 1 nC bunches with a frequency of 20 Hz. The energy spread will be 1% and the transverse emittance will be at most 10  $\mu\text{m}$ . The beam is then injected into the plasma channel (see also Section V).

### III. PLASMA SECTIONS

We now turn to the components that are based on plasma. We begin with a description of the electron bunch acceleration in plasma.

#### A. Proton-driven Plasma Wakefields

##### 1. Self-modulation stage

As discussed in Section IC, the long proton bunch delivered from the proton accelerator in Section IIA must be conditioned before it can drive wakefields suitable for the acceleration of a witness bunch of electrons. The plasma electrons react to the space charge of the proton bunch as it passes, resulting in a plasma wave. In the linear regime, where the amplitude of the wave is small compared to the cold wavebreaking limit  $E_c = mc\omega_p/e$ , the plasma response can be determined by the Green's function. Here,  $\omega_p = \sqrt{ne^2/\varepsilon_0 m}$  is the plasma frequency, with  $n$  the number density of the unperturbed plasma,  $-e$  and  $m$  the electron charge and mass,  $\varepsilon_0$  the vacuum permittivity and  $c$  the vacuum speed of light. In the co-moving frame,  $\tau = t - z/c$ , the on-axis accelerating field  $E_z$  is then given by:

$$E_z(\tau) = -\frac{k_p^2}{2\pi\varepsilon_0} \int_{-\infty}^{\tau} I_{\text{eff}}(\tau') \cos(\omega_p(\tau - \tau')) d\tau' \quad (1)$$

where  $k_p = \omega_p/c$  is the inverse plasma skin depth, and  $I_{\text{eff}}$  the effective current, a measure of the wakefield amplitude excited by each slice of the beam [21, 22]:

$$I_{\text{eff}}(\tau) = v_b \int_0^{\infty} r \rho_b(\tau, r) K_0(k_p r) dr, \quad (2)$$

with  $v_b \sim c$  the driver velocity,  $\rho_b$  the driver charge density, and  $K_0$  the modified Bessel function of the second kind. For the large-amplitude wakefields considered in this work, simulations are required to model the nonlinear response of the plasma and the evolution of the proton driver. However, linear theory remains a useful tool to understand the underlying processes. Simulations were carried out using the particle-in-cell code LCODE [23, 24].

The proton beam is focused to a waist size of 200  $\mu\text{m}$  at the entrance of the first plasma source consisting of rubidium vapour with a number density of  $7 \times 10^{14} \text{ cm}^{-3}$ . The ionizing laser co-propagates with the proton beam,  $1\sigma_z$  (170 ps) ahead of the bunch centroid. The portion of the beam propagating ahead of RIF is not subject to plasma wakefields, while the portion behind the RIF is periodically focused and defocused, leading to self-modulation. The RIF provides a fixed point in the co-moving frame from which self-modulation grows, providing a reproducible wakefield phase [18].

Figure 3a shows snapshots of the proton driver as it first enters the plasma and after 12 m of plasma propagation, at which point it is fully modulated. The wakefield excited by different

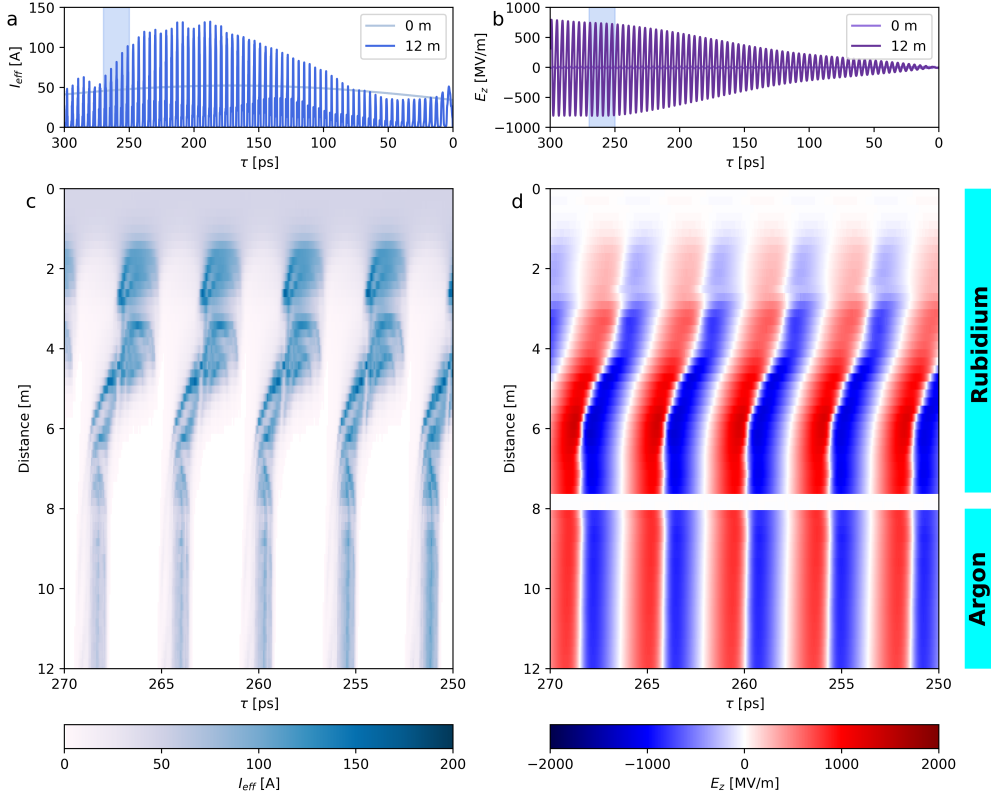


FIG. 3. a) The proton bunch profile and b) the associated longitudinal wakefield at the beginning of the first plasma and after 12 m of propagation. c) and d) The evolution of these quantities over the first plasma source and beginning of the second plasma source, showing self-modulation followed by phase stabilization. The  $\tau$  range in c, d correspond to the shaded areas in a, b.

slices of the unmodulated bunch interfere destructively, resulting in low wakefield amplitudes, as shown in Fig. 3b. Although these initial fields are too small to be suitable for acceleration, they are sufficient to periodically focus and defocus the proton bunch over a propagation distance of  $\sim 2$  m. The focused regions of the beam form microbunches, which have a much larger effective current than the defocused regions. The microbunches are periodic on the plasma frequency, and so their contributions sum coherently, resulting in wakefields of 800 MV/m after modulation.

As the wakefields grow, nonlinearities in the plasma response lead to a shift in the resonant plasma frequency. This results in a phase shift of the plasma wakefields which, if not corrected, leads to the microbunch train being defocused and a decrease in the wakefield amplitude. A plasma density step early in the self-modulation process allows the wakefield phase to be corrected [20]. The result is a train of microbunches which survive for long propagation distances [25, 26], allowing the acceleration of a witness bunch to high energy. For these parameters, a 4% density step after 0.5 m of plasma was chosen to stabilize the wakefields.

The phase of the microbunch train varies rapidly during self-modulation, as can be seen in Figs. 3c, d, which show the evolution of a section of the proton driver and the associated wakefields. A 30 cm gap is therefore introduced after 7.7 m of plasma, allowing a witness bunch of electrons to be injected into the phase-stable wakefields for acceleration.

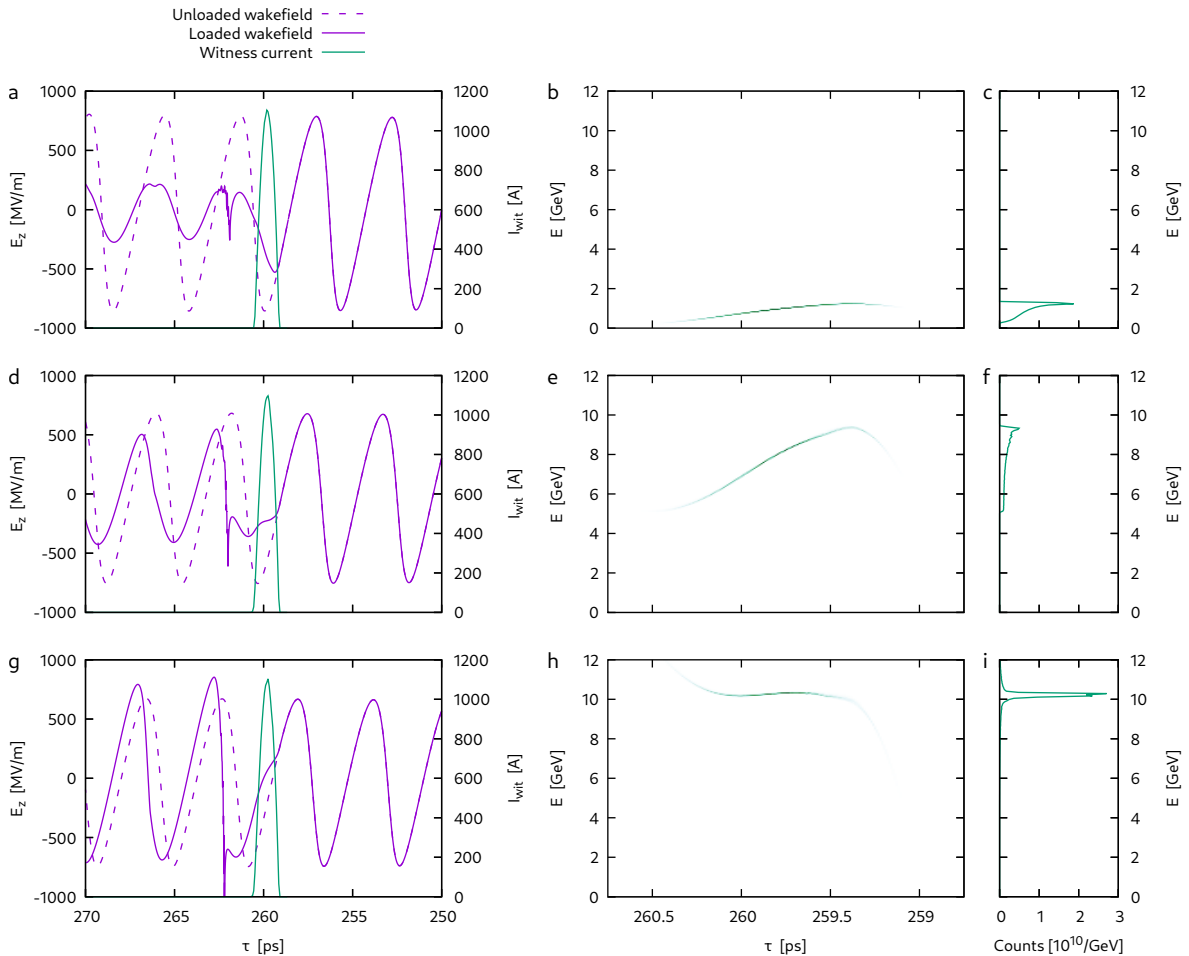


FIG. 4. a, d, g) the longitudinal wakefield acting on the electron bunch after 2, 25, and 50 m acceleration, respectively. The wakefields both in the absence (“unloaded”) and presence (“loaded”) of the 1 nC electron bunch are shown. b, e, h) the corresponding longitudinal phasespace and c, f, i) energy spectrum.

## 2. Acceleration stage

Acceleration of the electron bunch takes place in a second plasma with a length of 50 m. An argon discharge was chosen for this source, as discussed in Section III C. Figure 4a shows the electron bunch and the wakefields acting upon it after 2 m of plasma propagation. Although the modulated proton bunch excites wakefield amplitudes of  $\sim 800$  MV/m (the “unloaded” wake), the electron bunch also drives wakefields. In the accelerating phase, the wakes driven by the proton and electron bunches destructively interfere, with the electron bunch accelerated in the process.

The 1 nC electron bunch charge, necessary for the EIC injector, is much larger than that planned in the AWAKE experiment [2], and so the impact of beamloading is more significant. Beamloading can be seen in Fig. 4a, with the wakefields in the presence of the electron bunch (the “loaded” wake) significantly lower than the unloaded wake. The wakefields become strongly nonlinear after the passage of the electron bunch, consistent with the formation of a blowout [27].

The disparate masses of the protons and electrons results in bunches which propagate at different velocities. The electron bunch is essentially stationary in the light frame  $\tau$ , while the proton bunch and the wakefields it excites gradually fall backwards. Injection into the second plasma cell avoids

the rapid phase variation which occurs during the formation of the microbunch train, and the use of a density step in the first plasma results in wakefield amplitudes which remain essentially constant over the full acceleration length. However, the slow variation in the phase of the proton-driven wakefields due to the different bunch velocities remains, as seen by the varying wakefield phase in Figs. 4a,d,g, corresponding to 2, 25 and 50 m of plasma propagation. This dephasing is the main limitation on the acceleration length [26].

Figures 4b, e, h show the evolution of the longitudinal phasespace. The combined effect of dephasing and beamloading is that the loaded accelerating field sweeps through the electron bunch, with the head accelerated first, and then the tail. The longitudinal phasespace of the electron bunch develops a characteristic ‘s’-shaped profile during the acceleration, with the phasespace rotating over the acceleration length. The injection position and the electron bunch duration were chosen such that the energy spread, shown in Figs. 4c, f, i, is minimized after acceleration, with the head and tail reaching the same energy.

It can be seen from Fig. 4h that at end of the acceleration length, the loaded wakefield acting on the electron bunch head is decelerating, while that acting of the tail remains accelerating. The net energy transfer from the proton driven wake to the electron bunch approaches zero, with the amplitude of the plasma wave effectively unchanged by the electron bunch. However, these final stages of propagation in plasma act to de-chirp the electron bunch, resulting in a narrowly peaked final spectrum shown in Fig. 4i.

The 1 nC electron bunch is accelerated to 10 GeV in 50 m of plasma. The final bunch has a quasimonoenergetic energy spread typical of wakefield accelerators, with 63% of the bunch charge within  $\pm 1\%$  of the peak. The tails of the energy spectrum (the ends of the ‘s’) arise due to the longitudinal profile of the electron bunch, and can be removed through proper shaping of the current [28, 29]. Although beyond the scope of this work, shaping the electron bunch should also lead to an increase in efficiency, allowing the electron bunch charge to be increased.

## B. Plasma Acceleration of Polarized Electrons

A key requirement for the EIC electron injector is the preservation of the high degree of polarization provided by the conventional source during the subsequent plasma-based acceleration stage. For externally injected electron beams, this question can be addressed within the framework of spin dynamics in strong electromagnetic fields, governed by the Thomas–Bargmann–Michel–Telegdi (T-BMT) equation,

$$\frac{d\mathbf{s}}{dt} = -\boldsymbol{\Omega} \times \mathbf{s} . \quad (3)$$

Here,  $\mathbf{s}$  is the polarization vector and  $\boldsymbol{\Omega}$  the precession frequency

$$\boldsymbol{\Omega} = \frac{e}{mc} \left[ \Omega_B \mathbf{B} - \Omega_V \left( \frac{\mathbf{v}}{c} \cdot \mathbf{B} \right) \frac{\mathbf{v}}{c} - \Omega_E \frac{\mathbf{v}}{c} \times \mathbf{E} \right] , \quad (4)$$

with  $\mathbf{v}$  the particle velocity and  $\mathbf{E}, \mathbf{B}$  the electric/magnetic field. The prefactors in the above equation are given by

$$\Omega_B = a + \frac{1}{\gamma} , \quad \Omega_V = \frac{a\gamma}{\gamma + 1} , \quad \Omega_E = a + \frac{1}{\gamma + 1} , \quad (5)$$

and depend on the electron anomalous magnetic moment  $a = (g - 2)/2 \approx 10^{-3}$  and the Lorentz factor  $\gamma$ .

In a plasma wakefield accelerator, electrons experience strong transverse focusing fields and longitudinal accelerating fields, which in principle can induce spin precession and lead to depolarization. An overview of the general state-of-the-art is given by Reichwein *et al.* in [30]. Particle-in-cell simulations that include spin tracking [31, 32] show that depolarization effects are dominated by the injection phase, where electrons are still moderately relativistic,  $\gamma \ll 1/a$ , and may sample rapidly varying electromagnetic fields. In contrast, during the main acceleration stage, where electrons are accelerated from hundreds of MeV to multi-GeV energies and have  $\gamma \geq 1/a$ , the spin drift is suppressed. However, the spin direction of the highly relativistic electrons oscillates with the betatron period as the particles sample the focusing field of opposite direction at different betatron phases [33]. This effect causes spread in the bunch polarization as electrons populate all possible betatron phases. For a bunch of radius  $\sigma_r$  the polarization spread  $\Delta\mathbf{s}$  for longitudinally polarized electrons calculated in [33] is:

$$\frac{|\Delta\mathbf{s}|}{s_0} = \frac{1}{8\sqrt{2}} (1 + s_0^2) k_p^2 \sigma_r^2 \gamma a^2 \quad (6)$$

where  $s_0 = \mathbf{e}_z \cdot \mathbf{s}_0$  is the initial longitudinal polarization.

A matched electron bunch with normalized emittance  $\epsilon_n$  has an equilibrium radius

$$\sigma_r = k_p^{-1} \left( \frac{2}{\gamma} \right)^{1/4} (k_p \epsilon_n)^{1/2}. \quad (7)$$

Substituting (7) into (6), we obtain the general expression for the polarization spread of an electron bunch caused by plasma wakefields,

$$\frac{|\Delta\mathbf{s}|}{s_0} = \frac{1}{8} (1 + s_0^2) k_p \epsilon_n \gamma^{1/2} a^2. \quad (8)$$

This result has important implications for the present scheme. In the proposed EIC injector, electrons are externally injected from a conventional polarized source with an energy of 150 MeV and are rapidly accelerated to multi-GeV energies within the plasma stage. Since the injection process can be carefully controlled (e.g. via phase-stable injection into the wake), the main contribution to depolarization can be minimized. Once the electrons reach relativistic energies, subsequent acceleration to the final energy of 10–18 GeV occurs in a regime where spin precession effects are strongly suppressed. Taking the proposed EIC injector electron bunch parameters of  $\gamma = 2 \times 10^4$ ,  $\epsilon_n = 10 \mu\text{m}$ ,  $k_p^{-1} = 200 \mu\text{m}$  and  $s_0 = 0.85$ , we obtain the expected polarization spread caused by the plasma wakefield to be  $|\Delta\mathbf{s}|/s_0 \approx 1.5 \cdot 10^{-6}$ .

Overall, both analytical considerations and numerical studies indicate that polarization preservation in plasma wakefield acceleration is robust for externally injected, highly relativistic electron beams. Therefore, the high initial polarization ( $\sim 85\%$ ) provided by the source can be maintained throughout the plasma acceleration stage to a level compatible with the EIC requirements.

### C. Plasma cell concepts

The proposed scheme, shown in Fig. 9, closely follows the baseline design for AWAKE Run 2-D [2] and employs two distinct plasma sources. The first plasma induces self-modulation of the proton bunch into a train of microbunches that resonantly drive a wakefield in the second plasma section, which then accelerates a witness electron bunch [15]. A small gap between the two plasmas enables on-axis injection of the electron bunch into the wakefield using a magnetic dipole, which is essential for preserving beam quality.

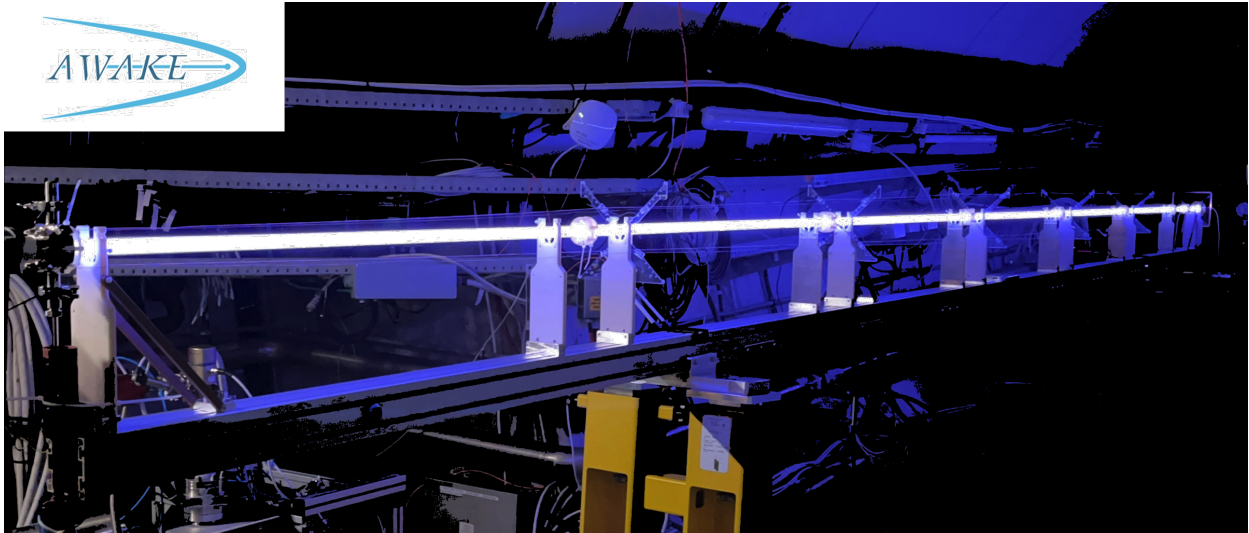


FIG. 5. Discharge plasma source (DPS) operating in the AWAKE experiment. The image shows the DPS configured as a single plasma column of 10 m length, with plasma generated in argon at 8 Pa using a 350 A peak-current heating pulse (courtesy of A. Sublet and the AWAKE team).

The requirement to inject the witness electron bunch at a reproducible wakefield phase (discussed above) constrains the first plasma to be generated by a laser-driven relativistic ionization front (RIF), synchronized with the electron bunch. The RIF, co-propagating with the leading edge of the proton bunch, provides a deterministic seed for its phase-locked self-modulation. Uniform-density plasmas with lengths of  $\sim 10$  m can be produced via field ionization of an alkali vapor using a short-pulse, high-intensity laser with a long focal length, with the vapor density precisely controlled through the temperature of the source vessel.

The alkali vapour plasma source developed for the AWAKE experiment [34] uses rubidium vapour. The choice of rubidium is motivated by its low first ionisation potential, the sufficiently large gap to the second ionisation potential, its relatively high ion mass, and the comparatively low temperature required for the vapour to reach the target densities ( $150^\circ\text{C}$  to  $250^\circ\text{C}$ ). Although the repetition rate considered here (20 Hz) is significantly higher than that of AWAKE (0.05 Hz), it remains compatible with the technological solution developed for this scheme.

The proposed RIF scheme directly impacts the beamline layout, as long-focal-length optics ( $\sim 50$  m) is required to produce plasma lengths of up to 10 m using a short-pulse ( $\sim 50$  fs) CPA laser with an energy of  $\sim 200$  mJ. This constrains the last mirror in the laser beamline to be placed at  $\sim 20$  m upstream of the first (rubidium vapor) plasma section, while leaving sufficient space to bend the proton beam trajectory towards the laser propagation axis using a dipole magnet.

The controllable plasma density step, adjustable in amplitude and axial position and required to enhance the accelerating gradient, can be implemented in the rubidium vapor source by imposing a corresponding temperature step using independently controlled heating sections along the plasma cell.

The second plasma section (accelerator plasma in Fig. 9) consists of a plasma with an electron density matching that of the preceding modulator plasma and extending over the required acceleration length (50 m in this case). Generating such a long plasma using laser field ionization of an alkali vapor would require a very high-power laser and impractically long focal-length optics. Therefore, closely following the AWAKE Run 2-D baseline design, we propose to use a length-scalable plasma source capable of producing a long preformed plasma column.

Two approaches are currently under development: helicon discharges (HPS) [35, 36] and direct

current discharges (DPS) [37–39]. We propose to use a DPS for the second plasma since it has been shown to generate plasma columns with lengths up to 10 m [39] and sufficient uniformity to self-modulate SPS 400 GeV proton bunches, in the AWAKE experiment, with results similar to the standard RIF method [40] (excluding phase-locking, since this is a preformed plasma and there is no SMI seeding). A photograph of the DPS generating a 10 m long plasma in argon is shown in Fig. 5.

DPS plasmas reach the target electron density using a short-pulse (a few microseconds), high-current density ( $\approx 100 \text{ kA cm}^{-2}$ ) discharge between electrodes located at the extremities of a long dielectric tube filled with low-pressure gas (2 Pa to 50 Pa). A low-jitter ignition of these short-pulse arc discharges is crucial for synchronizing the plasma discharge with the particle beams. We adopt a two-stage ignition-heating approach [38] in which both stages are direct-current arc discharges between a cold cathode and an anode immersed in the gas.

The initial discharge (ignition) is driven by a fast-rise-time high-voltage pulse (up to  $\approx 50 \text{ kV}$ ) generated by a flyback transformer that reliably initiates the plasma via cold electron emission at the cathode enhanced by the intensified electric field between the cathode and the current-return tube shield. This stage produces a diffuse and uniform plasma with a low ionization fraction (currents in the range 10 A to 50 A) along the tube. Higher ionization fractions ( $\sim 10\%$  to  $60\%$ , depending on the gas and pressure) are subsequently achieved using a lower-voltage (4 kV to 10 kV) efficient capacitive discharge (heating pulse).

The choice of gas is mainly constrained by the ion mass required for negligible ion motion that would otherwise reduce the wakefield amplitude within the proton bunch duration. This restricts the usable gases to those with ion masses greater than or equal to that of argon [40, 41].

The DPS was tested so far for plasma lengths of up to 10 m and is expected to perform well for longer lengths. However, since the heating pulse voltage needs to be proportional to the plasma tube length, significantly longer plasmas will require the combination of multiple discharges. The first step in length-scaling consists of producing two plasmas in a tube with two oppositely directed discharges originating from a common cathode, located at the tube midpoint and propagating towards anodes at the tube extremities. The currents in both plasmas are forced to be equal by a set of magnetic chokes that suppress current imbalance. Arbitrarily long plasma lengths can be achieved by combining these double plasma sections as schematically shown in Fig. 6 for a combination of four plasma sections.

A demonstration of a 12 m long plasma consisting of two double plasma sections (four plasma discharges in total, in a setup similar to the one shown in Fig. 6) has recently been performed. Preliminary results indicate that this method generated equal currents in the four plasma sections (to within 1%), essential for uniform length-scalable plasmas. When required, the fine tuning of the currents can be achieved by modifying the charging voltages in each pulse generator.

When needed, ionization fractions close to 100 % can be produced by combining a higher heating discharge current with a solenoid magnetic field ( $\sim 0.2 \text{ T}$  to  $1.0 \text{ T}$  depending on gas and plasma tube diameter). These magnetic fields are not expected to affect the wakefield and the acceleration process but instead mildly confine the plasma, reducing the energy transport to the tube walls. This results in an increase in plasma temperature and, consequently, the ionization fraction. For example, argon plasmas ionized above 90 % can be obtained with a current density of  $80 \text{ A cm}^{-2}$  and a solenoid magnetic field of  $0.7 \text{ T}$ . Using a high ionization fraction plasma can lead to increased plasma uniformity if a plateau in ionization fraction versus density current is reached since this reduces the dependence of the plasma density on the inner tube diameter tolerance. In this application, since the repetition rate allows for plasma full recombination, we aim for low current densities and ionization fractions ( $\sim 20\%$  in argon). This avoids the use of the solenoid magnetic field but imposes a strict tolerance of the dielectric tube diameter to ensure the requires current density uniformity.

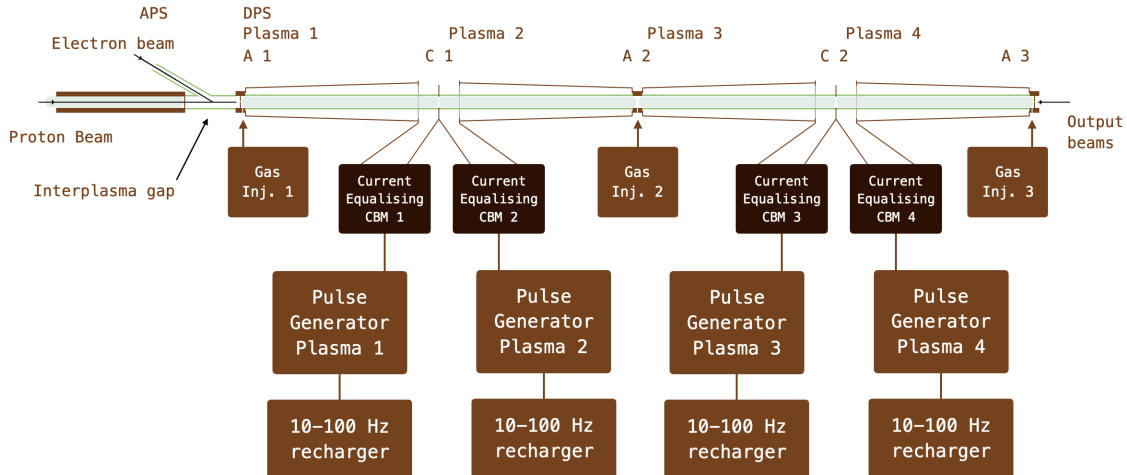


FIG. 6. Simplified scheme of discharge plasma source (DPS) consisting of four equal plasmas with a total length of 50 m (not in scale). The scheme also shows the end of the previous alkali plasma source (APS) and the interplasma gap - used for electron injection in the wakefield generated by the self-modulated proton bunch in the DPS plasma. This scheme can be used to produce arbitrarily long plasmas by joining additional double plasma sections. Each pulse generator produces the consecutive pulses to generate each plasma, current equalizing magnetic chokes are used to force equal currents in each plasma. The entire plasma source is required to be electrically isolated from adjacent metal parts with the grounding of each module to be made inside the respective pulse generator.

Although the proposed plasma sources are now relatively well tested, the detailed implementation of the two plasma sections scheme is still in the design phase within the AWAKE experiment. One of the main design priorities is the reduction of the interplasma gap length, which is required to enable on-axis injection of the witness electron beam into the wakefield of the second plasma. Longer free-propagation distances of the self-modulated proton bunch lead to a reduction in wakefield acceleration efficiency.

This interplasma region is densely populated with critical components, including the electron injection dipole, the downstream end of the alkali plasma source (comprising a laser beam dump and diagnostics of proton bunch self-modulation), and the upstream end of the second plasma (including a discharge anode that must be electrically isolated from surrounding components), as well as beam diagnostics for quality assessment and for alignment and synchronization of the proton and electron beams.

Precise temperature control is required in both plasma cells to ensure density uniformity and to generate controlled density steps and, if required, longitudinal density gradients to optimize the acceleration process. The proposed scheme is expected to operate in burst mode, with significant energy intermittently transferred from the proton beam to the plasma and surrounding structures. This may induce plasma density fluctuations due to non-uniform heating, cooling transients, and mechanical perturbations of the discharge tube. Therefore, a detailed thermal design is required for each implementation, taking into account repetition rate, duty cycle, beam energy, and energy transport to the walls. The thermal stability of the vapor or gas in the first and second plasma sources, which translates into plasma density uniformity, is especially important when using long proton bunches that self modulate into a large number  $N_b$  of microbunches with  $N_b \approx L_b/\lambda_{pe}$ , where  $L_b$  is the bunch length and  $\lambda_{pe}$  is the plasma wavelength. To prevent dephasing, the variations

of the plasma wavelength must be kept under  $\lambda_{pe}/4$  in the tail of the bunch, or  $\Delta\lambda_{pe}/\lambda_{pe} \leq \lambda_{pe}/(4L_b)$  which translates into  $\Delta n_e/n_e \leq \lambda_{pe}/(2L_b) \approx 1.6 \times 10^4/(L_b n_e^{1/2})$ . For  $L_b = 0.05$  m and  $n_e = 7 \times 10^{14} \text{cm}^{-3}$  we obtain  $\Delta n_e/n_e \leq 1.2\%$ .

The higher repetition rate, compared with AWAKE, imposes two additional changes on the DPS modules. The plasma ignition pulse, which in AWAKE is a sharp rise-time pulse with a long decay (triangular waveform), must now have short rise and fall times, since long pulses lead to longitudinal density modulations that may affect the plasma uniformity at 20 Hz. This problem can be avoided by changing the ignition circuit from a flyback transformer to a Marx bank topology. The second change is related to plasma ion drift. The plasma ions are accelerated along the tube from anode to cathode during the discharge. Keeping the heating pulses short (few microseconds) reduces the drift to  $\sim 1$  cm. Although this drift is negligible for a single pulse, at 20 Hz it may result in gas accumulation/rarefaction at cathode/anode regions. This problem can be circumvented, as in argon ion lasers, by a return tube that keeps the pressure equilibrium between cathodes and anodes. Alternatively, the ion drift can be compensated by using a second high-current pulse, with opposite polarity to the heating pulse, launched immediately after the end of the heating pulse and the beam propagation. This ion drift mitigation pulse in practice duplicates the plasma heating circuit but reduce the complexity of the plasma tube geometry by eliminating the gas return tube.

The upstream interface of the second plasma is critical for the quality of the accelerated beam. A thin metallic foil (used as the first discharge anode) can confine the gas, leading to improved density stability and plasma uniformity. However, propagation of the relatively low-energy witness electron beam through the foil may degrade beam quality. In that case, the foil must include an aperture for beam injection, and the gas injection system must compensate for the resulting gas losses. Differential pumping would then be required to maintain the upstream vacuum.

The baseline parameters of both plasma sections are summarized in Table IV.

Parameter	Units	Value
SMI Plasma Length	[m]	7
Acceleration Plasma Length (DPS)	[m]	50
Plasma Density	$10^{14}[\text{cm}^{-3}]$	7
Density Uniformity/reproducibility	%	$\leq 1.2$
DPS Tube Inner Diameter	mm	25
DPS Plasma Sections	-	4
DPS Plasma Section Length	[m]	12
DPS Heating Peak Current	[A]	800

TABLE IV. Design parameters of the plasma sources.

## IV. INJECTION INTO THE ELECTRON STORAGE RING

### A. Energy correction

Existing results [29] indicate that with the proper shaping of the electron witness bunch (triangular with sharp rising edge), it is possible to flatten the wakefield and achieve nearly constant accelerating field. Energy spreads of  $\approx 1\%$  should be possible with this witness bunch shaping. The centroid of the energy distribution will be affected by timing jitter of the injected electron bunch relative to the wakefield. As discussed, the electron bunch is prepared based on the ionizing laser pulse. This laser pulse initiates the modulation process and determines the timing of the generated wakefields. Based on expectations developed in the course of the AWAKE setup, we

anticipate timing jitters between the wakefields and electron bunch of at most 50 fs. This phase jitter will result in % level absolute energy jitter of the electron bunch.

The ESR beam is stable for up to 1 % energy oscillations [42], which has important implications for the allowed variations in the injection energy. If this margin is consumed by the combination of the injected bunch's energy spread and energy jitter, there is no transverse dynamic aperture left that is required to accommodate injection oscillations which are associated with beam accumulation. (Note the transverse dynamic aperture is close to zero at the energy acceptance level of  $\Delta E/E \simeq 1\%$ ). Thus, a scheme for correcting the energy spread and offset of the injected bunch is necessary. This could be realized as a chicane with an  $R_{56} = -0.131$  m, e.g., four 12 T m bending dipoles producing millimetre-scale path length differences over  $\sim 40$  m for energy variations on the % level. These path length differences would change the phase of the electrons entering an RF accelerating section providing a 100 MV/m of RF with a length of 6.4 m allowing energy differences of  $\approx 170$  MeV to be compensated. The phase-based corrector could be implemented as an X-band RF structure of a few 6.4 m length (assuming gradients of 100 MV/m). More precise values on the required distances, bending fields and RF voltage will require a more detailed investigation into the achievable energy spread and jitter for the electron bunches exiting the plasma section.

## B. Top-up Injection Scheme

At an energy of  $E = 10$  GeV, the Electron Storage Ring (ESR) in high luminosity operation stores  $n_b = 1160$  bunches with a charge of  $Q_b = 28$  nC. The electron bunch charge demonstrated in the plasma acceleration simulations in Section III A is only  $Q_b = 1$  nC. Thus the required electron bunch charge needs to be accumulated in the ESR.

For each proton driver cycle,  $n_p = 1160$  drive bunches are provided from the Blue-Ring. These bunches are extracted within a time that is short compared to the driver cycle time, with each drive bunch accelerating a 1 nC electron bunch. The finite electron lifetime in the ring means that somewhat more than 28 accumulations are required in order to reach 1160 electron bunches of 28 nC. Accumulations are spaced in time by 11 min, and so it takes more than  $28 \times 11 \text{ min} = 5 \text{ h}$  to complete the injection process. After the full bunch charge has been reached, it is maintained by adding an appropriate amount of charge in each refill cycle until the end of the storage period. The length of the store is limited by the time at which the proton bunches in the Hadron Ring of the EIC (HSR) are deteriorated to the extent that a new proton fill needs to be injected and accelerated in the HSR.

The electron bunch charge in the ESR is:

$$Q_b(t + \tau_{fill}) = Q(t) \cdot \exp\left(\frac{-\tau_{fill}}{\tau_e}\right) + \delta Q \quad (9)$$

where  $t$  is the time since the most recent injection,  $\tau_{fill}$  is the time between subsequent accumulation steps,  $\tau_e$  is the electron beam lifetime and  $\delta Q$  the electron charge added each accumulation step. The maximum charge supported by the plasma accelerator is injected each accumulation cycle until the full bunch charge has been reached. After this point, only the charge loss since the last fill need be injected,  $\delta Q = Q_b \exp(-t/\tau_e)$ .

The polarization  $P$  of the electron beam is another important performance parameter. The beam is injected with an initial polarization of  $P_0 = 85\%$ . The polarization of the stored beam without accumulation would be subject to depolarization with a decay constant of  $\tau_p$  until the asymptotic value of  $P_\infty$  is reached:

$$P(t) = P_\infty + (P_0 - P_\infty) \cdot \exp\left(\frac{-t}{\tau_p}\right) \quad (10)$$

Parameter	Units	10 GeV Value	18 GeV Value
Electron Energy	GeV	10	18
Maximum Bunch Charge in ring	nC	28	10.7
Number of bunches in ring		1160	290
Plasma accelerator bunch charge	nC	1	0.64
Average Time between accumulations	min	11	2.25
Electron Beam Lifetime	min	600	27.0
$P_0$	%	85	85
$\tau_{bks}$	min	699	33
$P_\infty$	%	50	50
$P_{bks}$	%	85.91	81
$\tau_p$	min	406	20.4
Storage Time	min	600	600

TABLE V. The relevant parameters achieved in the current version of our scheme for charge accumulation and polarization development for ESR operation at 10 GeV and 18 GeV.

The asymptotic polarization is the equilibrium of the Sokolov-Ternov polarization due to the average emission of synchrotron radiation photons and the depolarization due to the statistic nature of the emission of photons and corresponding sudden changes in the orbit of the electrons. The polarization lifetime  $\tau_p$  depends on the asymptotic polarization of and ideal accelerator ring  $P_{bks}$  and the corresponding polarization time  $\tau_{bks}$ ,  $\tau_p = \tau_{bks} \cdot P_\infty / P_{bks}$ . The polarization during the process of charge accumulation and charge maintenance is then given by the following recursion formula:

$$P(t + \tau_{fill}) = \frac{\left( P_\infty + (P(t) - P_\infty) \cdot \exp\left(\frac{-\tau_{fill}}{\tau_p}\right) \right) \cdot Q(t) \cdot \exp\left(\frac{-\tau_{fill}}{\tau_e}\right) + P_0 \cdot \delta Q}{Q(t) \cdot \exp\left(\frac{-\tau_{fill}}{\tau_e}\right) + \delta Q} \quad (11)$$

The parameters that govern the charge accumulation and the polarization development are given in Table V.

The corresponding ESR bunch charge accumulation and polarization development for the 10 GeV case are shown in Fig. 7. The average bunch charge is 19.3 nC, which is 69% of the EIC baseline design of 28 nC. The average polarization is 75.8% which exceeds the EIC performance goal by 8.2%.

For 18 GeV operation, only 290 bunches are stored in the ESR, and so each cycle of 1160 drive bunches allows four accumulations per ESR bunch. The bunch charge in the ESR is also reduced from the value at 10 GeV. However, in order to reach 18 GeV, the electron bunch charge from the plasma accelerator must also be reduced in order to decrease the beamloading. We estimate the attainable bunch charge by interpolating between the energy gain for the 10 GeV bunch and the integrated field in the unloaded case [26], and attain a value of 640 pC.

The ESR bunch charge accumulation and polarization development for the 18 GeV case are shown in Fig. 8. The average bunch charge is 6.16 nC which is 58% of the EIC baseline design. The average polarization is 65.8% which is close to the EIC performance goal of 70%. The same optimizations as discussed for the 10 GeV case can be applied.

The studied injection scheme is close to the EIC performance requirement but these results are achieved only for antiparallel spin w.r.t. the guide field. As both longitudinal spin orientations are mandatory to suppress systematic errors, the electron spin rotators that rotate the vertical spin into longitudinal spin (and vice versa after collisions) must switch polarity at subsequent stores.

While these results fall somewhat short of the EIC performance requirements, it should be pointed out that there is quite some room for further improvement of the parameters of the plasma

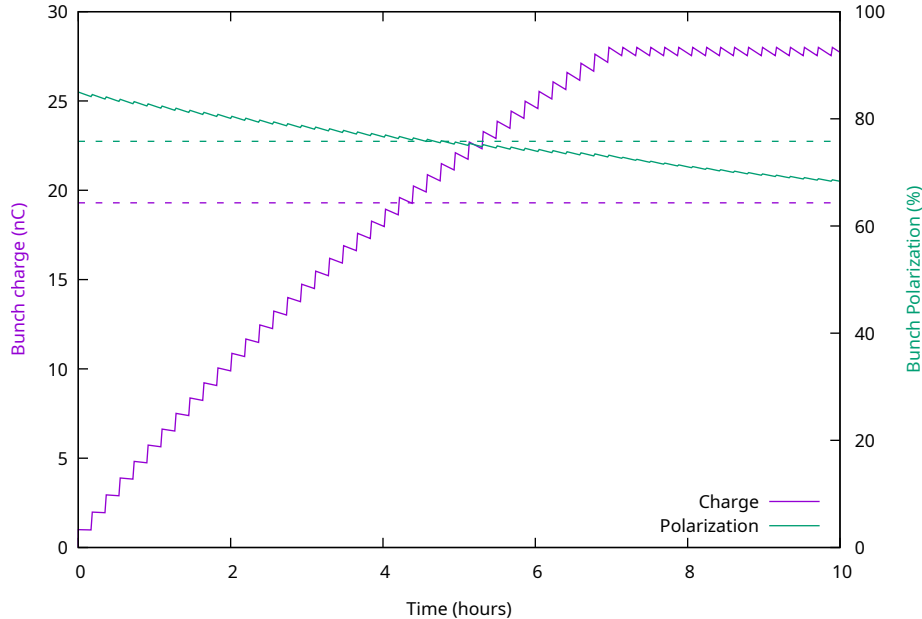


FIG. 7. Accumulation of bunch intensity and corresponding polarization development over the store time of  $\tau_{store} = 10$  h at 10 GeV. The average values over the store time are shown by dashed lines, with an average bunch charge of 19.3 nC, and an average polarization of 75.8%.

wakefield acceleration and an increase of the charge of the witness bunch appears to be an achievable goal. The calculations of average intensity and average polarization have been repeated for an increased charge of the accelerated electron beam. At 10 GeV, accelerating 2 nC of charge per drive bunch allows the full charge of 28 nC to be reached after 2.56 h and the corresponding average bunch charge increases to 24.1 nC, which is 86% of the performance goal. This is a significant improvement compared to the case with only 1 nC charge of the witness bunch. The average polarization of 74% remains above the performance goal.

In the 18 GeV case, doubling the electron charge per drive bunch to 1.28 nC increases the ESR bunch to 8.8 nC, 82% of the baseline value, while the average polarization is 65.7%, slightly less than in the case of  $\Delta Q_b = 640$  pC.

It should be pointed out that in all cases, the average bunch intensity can be increased at the expense of the polarization by increasing the electron lifetime. This trade-off can be optimized keeping in mind that the effective luminosity scales linearly the bunch charge but quadratically in polarization. It is also possible to operate with large electron lifetime during accumulation and a reduced lifetime when the full bunch charge has been reached. We therefore expect that further improvements may be possible.

## V. POTENTIAL LAYOUT

A schematic of the different elements is shown in Fig. 9. Proton drive bunches (blue line) are extracted from the Blue-Ring and transported to the plasma acceleration section. As mentioned in Section IC, the bunch has to be modulated, before it can be used for acceleration. The drive beam modulator consists of a 7.7 m-long, laser-ionized plasma (shown in light blue). A high-power laser pulse (red line) will need to be co-propagated with the incoming proton bunch, to create the plasma and seed the Self-Modulation process. At the exit of the modulator, a laser dump will be

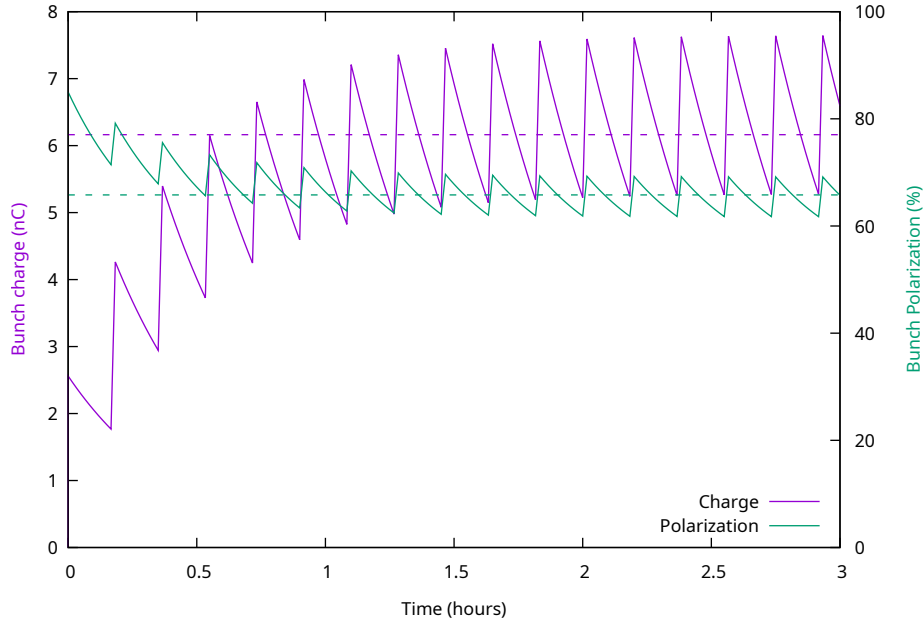


FIG. 8. Accumulation of bunch intensity and corresponding polarization development at 18 GeV. The average values over the full store time  $\tau_{store} = 10$  h are shown by dashed lines, with an average bunch charge of 6.16 nC and an average polarization is 65.8%.

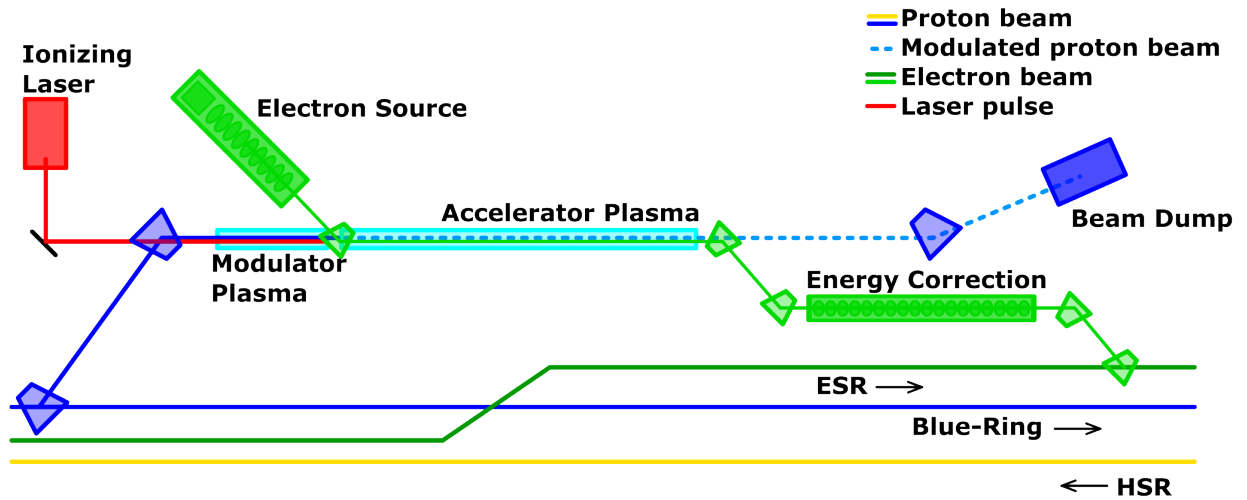


FIG. 9. Possible Layout: not to scale. Outline of the necessary beams is shown: proton beam in blue, electron beam in green, laser beam in red. The proton beam self-modulates while passing through the first plasma cell.

installed to stop the laser pulse. After the modulator plasma there is a 30 cm gap, which provides the necessary space for beam merging, and on-axis electron injection. Electron witness bunches (green line) are generated by a polarized electron source, and pre-accelerated to 150 MeV using a conventional linac. The beam is then transported to the plasma acceleration section, and injected into the second plasma in the 30 cm gap. The accelerator cell uses a discharge plasma source, and is expected to be approximately 50 m long.

Following acceleration, the proton drive beam is separated from the electron beam, and directed

to a proton beam dump. The accelerated electron bunches will be transported through an energy spread correction section, where their energy spread will be reduced to 1% to match the energy acceptance of the storage ring. The electron beam would then be injected into the storage ring. The plasma cells occupy a total of 58 m, leaving space for electron beam injection, diagnostics, and energy correction.

The compatibility of such a layout with existing infrastructure will require a detailed investigation. At present, it appears that an available space of  $\approx 200$  m will be sufficient to accommodate the different components.

## VI. DISCUSSION AND CONCLUSION

The scheme outlined in the previous sections indicates that EIC electron injector parameters are within reach for a scheme based on proton-driven plasma wakefield acceleration. We find that acceleration of an electron bunch of 1 nC ( $6 \cdot 10^{10}$  electrons) to 10 GeV is possible with a proton bunch of  $3 \cdot 10^{11}$  protons of 275 GeV. Reaching higher electron energies would require to reduce the electron bunch charge, but it is also a requirement of the EIC to reduce the electron bunch charge at the highest energies due to synchrotron radiation energy losses in the electron storage ring. An average rate of accelerated electron bunches to inject into the storage ring of  $> 1$  Hz is feasible when extracting proton bunches from the Blue-Ring at tens of Hz and refilling the proton ring within 11 minutes. Tens of Hz operation is not expected to be a problem for the plasma sections or for the polarized electron source. Topping-up the electron bunches in the storage ring at this rate will allow for a high average polarization ( $\geq 70$  %) which is critical for the EIC physics program. The proposed layout indicates that a 200 m straight section would be sufficient for the scheme.

A number of aspects still need to be verified, such as the  $< 1$  % energy spread required for injection into the electron storage ring, including the deviation from the nominal energy, after acceleration. Achieving this low level of energy spread will likely require the development of a novel electron linac capable of producing tailored longitudinal profiles for injection into the plasma. It will also likely require the development of a final corrector section based on standard RF technology which would be located after the plasma acceleration system to center the electron bunch energy on the desired energy. These two RF sections will need careful design and detailed studies. Given that they can be realized, the total accelerating voltage expected to be needed for producing and shaping the electron bunch before the plasma acceleration and for correcting the energy after the plasma is below 500 MV, which is below the value for the current EIC injector design. Given that the booster ring for the electron bunches would not be necessary, we anticipate that our scheme would be much less costly than the current scheme.

Developing an injector based on proton-driven plasma wakefields such as the one we describe would have an exciting additional benefit of demonstrating a new technology. This could become important for future nuclear and particle physics applications. The AWAKE experiment underway at CERN provides a valuable testing ground for many of the aspects of the scheme that are most challenging, including the electron bunch injection into the modulated proton bunch, the subsequent acceleration to high energies in the plasma while controlling the emittance of the electron bunch, and the development of plasma sources with the required uniformity over the needed distance scales. We conclude that resources should be dedicated for a fuller investigation of an electron injection system for the EIC based on proton-driven plasma wakefield acceleration.

## REFERENCES

- [1] F. Willeke and J. Beebe-Wang, *Electron Ion Collider Conceptual Design Report 2021*, Tech. Rep. (Brookhaven National Laboratory (BNL), Upton, NY, United States; Thomas Jefferson National Accelerator Facility (TJNAF), Newport News, VA, United States, United States, 2021).
- [2] E. Gschwendtner, K. Lotov, P. Muggli, M. Wing, *et al.* (AWAKE Collaboration), The AWAKE Run 2 programme and beyond, *Symmetry* **14**, 1680 (2022).
- [3] V. N. Litvinenko, N. Bachhawat, J. C. Brutus, L. Cultrera, K. Decker, M. Gaowei, P. Inacker, Y. Jing, J. Ma, K. P. Mondal, G. Narayan, I. Pinayev, F. Severino, K. Shih, J. Skaritka, L. Smart, Y. Than, J. Walsh, E. Wang, G. Wang, and D. Weiss, Towards advanced polarized electron sources, *Nature Physics* **22**, 325–330 (2026).
- [4] T. Tajima and J. M. Dawson, Laser electron accelerator, *Phys. Rev. Lett.* **43**, 267 (1979).
- [5] P. Chen, J. M. Dawson, R. W. Huff, and T. Katsouleas, Acceleration of electrons by the interaction of a bunched electron beam with a plasma, *Phys. Rev. Lett.* **54**, 693 (1985).
- [6] I. Blumenfeld *et al.*, Energy doubling of 42 GeV electrons in a metre-scale plasma wakefield accelerator, *Nature* **445**, 741 (2007).
- [7] A. J. Gonsalves *et al.*, Petawatt Laser Guiding and Electron Beam Acceleration to 8 GeV in a Laser-Heated Capillary Discharge Waveguide, *Phys. Rev. Lett.* **122**, 084801 (2019).
- [8] F. Albert, M. E. Couprie, A. Debus, M. C. Downer, J. Faure, A. Flacco, L. A. Gizzi, T. Grismayer, A. Huebl, C. Joshi, M. Labat, W. P. Leemans, A. R. Maier, S. P. D. Mangles, P. Mason, F. Mathieu, P. Muggli, M. Nishiuchi, J. Osterhoff, P. P. Rajeev, U. Schramm, J. Schreiber, A. G. R. Thomas, J.-L. Vay, M. Vranic, and K. Zeil, 2020 roadmap on plasma accelerators, *New Journal of Physics* **23**, 031101 (2021).
- [9] A. Caldwell, K. Lotov, A. Pukhov, and F. Simon, Proton Driven Plasma Wakefield Acceleration, *Nature Phys.* **5**, 363 (2009), arXiv:0807.4599 [physics.acc-ph].
- [10] J. Farmer, A. Caldwell, and A. Pukhov, Preliminary investigation of a higgs factory based on proton-driven plasma wakefield acceleration, *New Journal of Physics* **26**, 113011 (2024).
- [11] F. Willeke, *Study of a Fixed Field Accelerator as a Driver for Proton Driven Plasma Wakefield Acceleration*, Tech. Rep. (Brookhaven National Lab, 2026).
- [12] N. Kumar, A. Pukhov, and K. Lotov, Self-modulation instability of a long proton bunch in plasmas, *Phys. Rev. Lett.* **104**, 255003 (2010), arXiv:1003.5816 [physics.plasm-ph].
- [13] R. Assmann *et al.* (AWAKE Collaboration), Proton-driven plasma wakefield acceleration: a path to the future of high-energy particle physics, *Plasma Phys. Control. Fusion* **56**, 084013 (2014), arXiv:1401.4823 [physics.acc-ph].
- [14] A. Caldwell *et al.*, Path to AWAKE: Evolution of the concept, *Nucl. Instrum. Meth. A* **829**, 3 (2016), arXiv:1511.09032 [physics.plasm-ph].
- [15] P. Muggli *et al.* (AWAKE Collaboration), AWAKE readiness for the study of the seeded self-modulation of a 400 GeV proton bunch, *Plasma Phys. Control. Fusion* **60**, 014046 (2017), arXiv:1708.01087 [physics.plasm-ph].
- [16] L. Verra *et al.* (AWAKE Collaboration), Controlled Growth of the Self-Modulation of a Relativistic Proton Bunch in Plasma, *Phys. Rev. Lett.* **129**, 024802 (2022), arXiv:2203.13752 [physics.plasm-ph].
- [17] E. Adli *et al.* (AWAKE Collaboration), Acceleration of electrons in the plasma wakefield of a proton bunch, *Nature* **561**, 363 (2018), arXiv:1808.09759.
- [18] F. Batsch *et al.* (AWAKE Collaboration), Transition between Instability and Seeded Self-Modulation of a Relativistic Particle Bunch in Plasma, *Phys. Rev. Lett.* **126**, 164802 (2021), arXiv:2012.09676 [physics.plasm-ph].
- [19] K. V. Lotov, Controlled self-modulation of high energy beams in a plasma, *Phys. Plasmas* **18**, 024501 (2011).
- [20] K. V. Lotov, Physics of beam self-modulation in plasma wakefield accelerators, *Phys. Plasmas* **22**, 103110 (2015), arXiv:1503.05104 [physics.plasm-ph].
- [21] T. Katsouleas, S. Wilks, P. Chen, J. M. Dawson, and J. J. Su, Beam Loading in Plasma Accelerators, *Part. Accel.* **22**, 81 (1987).
- [22] R. Keinigs and M. E. Jones, Two-dimensional dynamics of the plasma wakefield accelerator, *Phys. Fluids* **30**, 252 (1987).
- [23] K. V. Lotov, Fine wakefield structure in the blowout regime of plasma wakefield accelerators, *Phys.*

- Rev. ST Accel. Beams **6**, 061301 (2003).
- [24] See <https://lcode.info> for code description and manual.
  - [25] K. V. Lotov and P. V. Tuv, Plasma wakefield acceleration beyond the dephasing limit with 400 GeV proton driver, *Plasma Phys. Controlled Fusion* **63**, 125027 (2021).
  - [26] H. Jaworska *et al.*, A full-energy electron injector for the EIC based on proton-driven plasma-wakefield acceleration, in *Proceedings of the 17th International Particle Accelerator Conf. (IPAC'26)*, TUP3043, in preparation.
  - [27] J. B. Rosenzweig, G. Andonian, M. Ferrario, P. Muggli, O. Williams, V. Yakimenko, and K. Xuan, Plasma wakefields in the quasi-nonlinear regime, *AIP Conference Proceedings* **1299**, 500 (2010), <https://aip.scitation.org/doi/pdf/10.1063/1.3520373>.
  - [28] S. van der Meer, *Improving the power efficiency of the plasma wakefield accelerator*, Tech. Rep. (CERN, Geneva, 1985).
  - [29] C. A. Lindström *et al.*, Energy-Spread Preservation and High Efficiency in a Plasma-Wakefield Accelerator, *Phys. Rev. Lett.* **126**, 014801 (2021).
  - [30] L. Reichwein, Z. Gong, C. Zheng, L. L. Ji, A. Pukhov, and M. Büscher, Plasma acceleration of polarized particle beams, *Reports on Progress in Physics* **88**, 117001 (2025).
  - [31] Y. Wu, L. Ji, X. Geng, Q. Yu, N. Wang, B. Feng, Z. Guo, W. Wang, C. Qin, X. Yan, L. Zhang, J. Thomas, A. Hützen, M. Büscher, T. P. Rakitzis, A. Pukhov, B. Shen, and R. Li, Polarized electron-beam acceleration driven by vortex laser pulses, *New Journal of Physics* **21**, 073052 (2019).
  - [32] Y. Wu, L. Ji, X. Geng, Q. Yu, N. Wang, B. Feng, Z. Guo, W. Wang, C. Qin, X. Yan, L. Zhang, J. Thomas, A. Hützen, A. Pukhov, M. Büscher, B. Shen, and R. Li, Polarized electron acceleration in beam-driven plasma wakefield based on density down-ramp injection, *Phys. Rev. E* **100**, 043202 (2019).
  - [33] J. Vieira, C.-K. Huang, W. B. Mori, and L. O. Silva, Polarized beam conditioning in plasma based acceleration, *Phys. Rev. ST Accel. Beams* **14**, 071303 (2011).
  - [34] G. Plyushchev *et al.*, A rubidium vapor source for a plasma source for AWAKE, *J. Phys. D: Appl. Phys.* **51**, 025203 (2018).
  - [35] B. Buttenschön *et al.*, A high power, high density helicon discharge for the plasma wakefield accelerator experiment AWAKE, *Plasma Phys. Control. Fusion* **60**, 075005 (2018).
  - [36] M. Granetzny *et al.*, Exploration of helicon plasmas for wakefield accelerators at the Madison AWAKE Prototype, *Physics of Plasmas* **32**, 093507 (2025).
  - [37] N. C. Lopes, C. Cobo, J. B. Ben Chen, P. B. Jury, L. C. Kennedy, A. Vanstone, and Z. Najmudin, A metre-scale plasma discharge for plasma wakefield acceleration, *Plasma Phys. Control. Fusion* **68**, 045046 (2026).
  - [38] N. E. Torrado, N. C. Lopes, J. F. A. Silva, C. Amoedo, and A. Sublet, Double pulse generator for unipolar discharges in long plasma tubes for the awake experiment, *IEEE Trans. Plasma Sci.* **51**, 3619 (2023).
  - [39] N. E. Torrado, C. Amoedo, A. Sublet, M. Taborrelli, S. F. Pinto, J. F. Silva, and N. Lopes, Double pulse generator for awake scalable discharge plasma source, *J. Phys.: Conf. Ser.* **3124**, 012021 (2025).
  - [40] M. Turner, E. Walter, C. Amoedo, N. E. Torrado, N. C. Lopes, A. Sublet, *et al.*, Experimental observation of the motion of ions in a resonantly driven plasma wakefield accelerator, *Phys. Rev. Lett.* **134**, 155001 (2025).
  - [41] J. Vieira, R. A. Fonseca, W. Mori, and L. O. Silva, Ion motion in self-modulated plasma wakefield accelerators, *Phys. Rev. Lett.* **109**, 145005 (2012).
  - [42] Y. Nosochkov *et al.*, Dynamic aperture of the EIC electron storage ring, *JACoW IPAC2024*, MOPC82 (2024).